Theoretical study of the effect of $(CdS)_{1-x}(ZnS)_x$ buffer layer on the performance of CIGS solar cells

SH. S. ALI[1], MAHROUS R. AHMED[1], W. S. MOHAMED[1,2], H. A. MOHAMED[1,*]
[1]*Physics department, Faculty of Science, Sohag University, 82524 Sohag, Egypt*
[2]*Physics Department, College of Science, Jouf University, Al-Jouf, Sakaka, P.O. Box 2014, Saudi Arabia*

Photovoltaic solar cell is one of the most important renewable energy sources. Solar cells based on thin-film layers are considered as promising photovoltaic and offer a number of interesting advantages compared to the bulk silicon devices. In all thin-film solar cells, CdS layer is applied as a heterojunction partner with CdTe, $CuInS_2$ and $CuInGaS_2$ (CIGS). Adding wide bandgap materials such as ZnS to CdS can led to increase the energy gap of CdS and allow more photons in short wavelength to pass through it and reach the absorber layer. In this work, the effect of $(CdS)_{1-x}$:$(ZnS)_x$(x=0, 0.1, 0.2, 0.3, 0.4 and 0.5) on the performance of CIGS solar cells are studied theoretically. The short-circuit current density (J_{SC}), open-circuit voltage (V_o), fill factor (*FF*) and the cell efficiency (η) have been estimated. The optical and recombination losses have been taken into consideration. Adding ZnS to CdS leads to a significant improvement in the performance of CIGS solar cells. Our results show that at x-ratio equals 0.5, the J_{SC} increases by 18% and the optical losses decrease by more than 25%. The optical losses have significant effect on J_{SC} more than the effect of recombination losses. The CIGS efficiency increases from 14.7% to 17.72% for x=0 and x=0.5, respectively.

(Received February 13, 2021; accepted August 10, 2023)

Keywords: CdS, ZnS, CIGS, Thin-film solar cells, Optical losses, Recombination losses

1. Introduction

Global energy production, both in quantity and source, has been changed dramatically over the ages. Using fossil fuels such as coal, crude oil and natural gas for the energy supply that will lead to the quick depletion of natural resources in the near future. Moreover, when these fuels are used for the production of energy, large amounts of greenhouse gases are inevitably emitted and pollute the environment. All these have urged us to explore alternative clean energy sources for sustainable human activities [1]. Renewable energy resources include solar energy, wind, hydropower, the heat of the earth (geothermal), plant materials (biomass), waves, energy of ocean and the energy of the tides [2-5]. Solar-electric power can be produced either by power plants using the sun's heat or by photovoltaic (PV) technology, which converts sunlight directly to electricity using solar cells. At present, photovoltaic solar cells are one of the most important renewable energy sources [6-8]. Most modern solar cells are made from either crystalline silicon or thin-film semiconductor material. Silicon cells are more efficient at converting sunlight to electricity, but generally have higher manufacturing costs [9]. Solar cells based on thin-film layers such as CdTe, Cu(In, Ga)Se_2 (CIGS) and $Cu_2ZnSn(S,Se)_4$ (CZTSSe) are considered promising photovoltaic and offers a number of interesting advantages compared to the bulk silicon devices [10]. CIGS material has unique properties such as high absorption coefficient ($>10^4$ cm^{-1}) and appropriate optical band gap (1.04:1.67 eV) [11, 12]. The conversion efficiency of the typical structure of substrate CIGS solar cell consists of ZnO:Al/CdS/CIGS/MO/Glass can reach 22% [13] and in modules is in the range12-15 % [14]. On the other hand, the theoretical limit of these solar cells is high and can reach 28-30% [14]. In all thin-film solar cells, CdS thin film is applied as a heterojunction partner with CdTe [15], $CuInS_2$ [16] and $CuInGaS_2$ [17]. However, CdS has relatively low energy gap (2.42 eV), hence the photons with energy higher than 2.42 eV may be absorbed by the CdS layer before reaching the absorber layer. One of the ways that can increase the energy gap for these materials is to add wide band gap materials such as ZnS [18]. The wide band gap of 3.7 eV of ZnS can allow more photons in short wavelength to pass through it [19].

Theoretical work plays a vital role in developing solar cells by providing a deeper understanding of their underlying principles, aiding in device design and optimization, enabling the discovery of new materials, and guiding experimental efforts. It is an essential complement to experimental work, accelerating progress and driving innovation in solar cell technology.

A trial has been carried out where, the thermal evaporation technique was employed to obtain thin films of $(CdS)_{1-x}$ $(ZnS)_x$ (x=0, 0.1, 0.2, 0.3, 0.4 and 0.5) and the optical and the structural properties of these films were studied [20]. In this work, the effect of $(CdS)_{1-x}(ZnS)_x$ on the performance of CIGS solar cells has been studied theoretically. The short-circuit current density, open-circuit voltage, fill factor and the cell efficiency have been estimated. The calculations of these parameters are carried out on the basis of the optical properties of (CdS):(ZnS) layer with different ZnS contents. The optical and recombination losses that can take place in these cells have been taken into consideration.

2. Theoretical model

In our model, CIGS is used as a p-type absorber layer and a thin layer of 150 nm of n-type CdS doped with different ratios of ZnS is used as a buffer layer to form a heterojunction with the absorber. A transparent conducting oxide (TCO) such as ZnO:AL of energy gap 3.3 eV is used as a charge-collecting layer. In addition, the spectrum was set to the global Am 1.5 standard and the operation temperature was maintained at 300 K. The other parameters namely thickness of ZnO:AL ($d_{ZnO:AL}$), thickness of CIGS (d_{CIGS}), width of space charge region (W), the barrier height(φ_0), the elementary charge (q), the velocity of recombination at the front surface of CIGS (S_f), the recombination velocity at the back surface of CIGS (S_b), the mobility of charge ($\mu_{n,\ p}$), and the lifetime of charge ($\tau_{n,\ p}$), used in this model are listed in Table 1.

Table 1. Parameters values used in the model

parameter	$d_{ZnO:Al}$ (nm)	d_{CIGS} (µm)	W (µm)	φ_0-qv (eV)	S_f (cm/s)	S_b (cm/s)	$\mu_{n,\ p}$ cm²/(V s)	$\tau_{n,\ p}$ (S)
Value	100	2	0.5	1	10^6	10^6	10^3	4×10^{-8}

Fig. 1 shows the schematic structure of CIGS solar cell. This model takes into account the optical losses result from the reflection at various interfaces and the absorption in TCO and buffer layers. Moreover, the recombination losses at both the front and back surface of CIGS have been studied. The reflectivity (R) at two adjusting layers 1 and 2 is determined based on the well-known Fresnel equations [21]:

$$R_{12} = \left(\frac{n_1^* - n_2^*}{n_1^* + n_2^*}\right)^2 \tag{1}$$

In case of electrically conductive materials, the refractive index (n^*) contains an imaginary part in addition to real part and is written as [22]:

$$n^* = n - ik \tag{2}$$

where n_1 is the refractive index of the first material, n_2 is the refractive index of the second material and k is the corresponding extinction coefficients. Therefore, the reflection coefficient, R, is written as

$$R_{12}(\lambda) = \frac{|n_1^* - n_2^*|^2}{|n_1^* + n_2^*|^2} = \frac{(n_1 - n_2)^2 + (k_1 - k_2)^2}{(n_1 + n_2)^2 + (k_1 + k_2)^2} \tag{3}$$

The experimental values of n and k of ZnO:AL, CdS:ZnS and CIGS were taken from the literature data [23, 20 and 14, respectively]

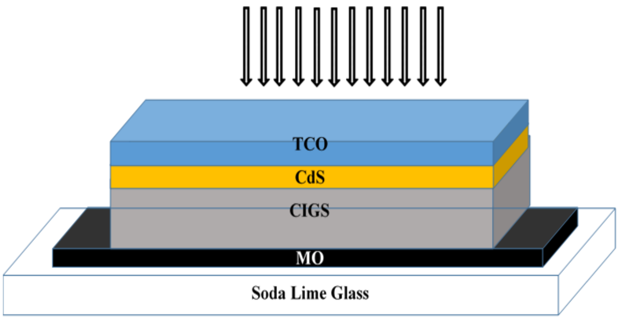

Fig. 1. Schematic structures of thin-film solar cells based on CIGS (color online)

The transmission in this case is given by:

$$T(\lambda) = (1 - R_{12})(1 - R_{23})(1 - R_{34}) \tag{4}$$

where R_{12}, R_{23} and R_{34} are the reflectivity at the interface between air/ZnO:AL, ZnO:AL/CdS:ZnS and CdS:ZnS/CIGS, respectively.

The absorption process is the second process that contributes in the optical losses and it takes place in TCO and n-type layers. In this case, Eq.4 takes the form [21]:

$$T(\lambda) = (1 - R_{12})(1 - R_{23})(1 - R_{34})e^{-\alpha_1 d_1}e^{-\alpha_2 d_2} \tag{5}$$

where, α_1 and α_2 are the absorption coefficient of ZnO:AL and CdS:ZnS, respectively and d_1 and d_2 are their thickness.

The internal quantum efficiency η_{int} of the solar cells consists of the drift and diffusion components. The photogeneration of electron-hole pairs in the space-charge region represents the drift component, while photogeneration of electron-hole pairs in the neutral part of the diode structure represents the diffusion component.

The drift component of the internal quantum efficiency (η_{drift}) is given from the solution of the continuity equation in the form [24, 25]:

$$\eta_{drift} = \frac{1+(S_f/D_p)[\alpha+(2/W)(\varphi_o-qV)/kT]^{-1}}{1+(S_f/D_p)[(2/W)(\varphi_o-qV)/kT]^{-1}} - \exp(-\alpha W) \quad (6)$$

where, S_f is the velocity of recombination at the front surface of CIGS, D_p is the hole's diffusion coefficient and it is related to the mobility μ_p by the Einstein relation $qD_p/kT = \mu_p$, α is the absorption coefficient of CIGS, W is the width of space-charge region, V is the applied voltage, and φ_o is the barrier height.

The diffusion component of the internal quantum efficiency (η_{dif}) is also given from the solution of the continuity equation [26]. The solution of the continuity equation was simplified with sufficient accuracy and can be written in the form [27],

$$\eta_{dif} = \frac{\alpha L_n}{\alpha^2 L_n^2 - 1}\exp(-\alpha W) \times \left\{\alpha L_n - \frac{\left(\frac{S_b L_n}{D_n}\right)[\cosh((d-W)/L_n) - \exp(-\alpha(d-W))] + \sinh((d-W)/L_n) + \alpha L_n \exp(-\alpha(d-W))}{\left(\frac{S_b L_n}{D_n}\right)\sinh[(d-W)/L_n] + \cosh[(d-W)/L_n]}\right\} \quad (7)$$

where, D_n is the diffusion coefficient of the electrons related to the mobility μ_n by Einstein relation $qD_n/kT=\mu_n$, L_n $(=(\tau_n D_n)^{1/2})$ is diffusion length of minority carriers, τ_n is the lifetime of electron, d is the absorber layer thickness and S_b is the recombination velocity at the back surface of CIGS.

From Eq. (6) and Eq. (7), the total internal quantum efficiency with recombination losses at front and back surface of the absorber layer is:

$$\eta_{int} = \eta_{drift} + \eta_{dif} \quad (8)$$

The contribution of transmittance (T) and internal quantum efficiency (η_{int}) on the short-circuit current density (J_{SC}) can be calculated according to the following formula [28]:

$$J_{SC} = q\sum_i T(\lambda)\frac{\Phi_i(\lambda_i)}{h\nu_i}\eta_{int}(\lambda_i)\Delta\lambda_i \quad (9)$$

where, Φ_i is the spectral power density, $\Phi_i/h\nu$ is the spectral distribution of the photons, $h\nu$ is the photon energy, $\Delta\lambda$ is the interval between neighbouring values of the wavelength, $T(\lambda)$ is given by Eq. (5) and $\eta_{int}(\lambda)$ is given by Eqs. (6, 7 and 8). The summation in Eq. (9) should be compute over the spectral range from λ=300 nm to $\lambda=\lambda_g=hc/E_g$, where E_g is the optical band gap of CIGS.

The optical and/or recombination losses can be determined using Eq. (9) and the flowing expression:

$$Losses\ (\%) = \left(1 - \frac{J_{SC}}{J_{SC\,(max)}}\right) \times 100 \quad (10)$$

where $J_{SC\,(max)}$ is the maximum short-circuit current density obtained at $T(\lambda)=1$ and/or $\eta_{int}(\lambda)=1$.

According to the standard diode equation, the J(V) characteristic of a single-junction solar cell under illumination can be written as the linear superposition of the dark characteristics of the cell and the photogenerated current:

$$J = J_0\left[\exp\left(\frac{qv}{AkT}\right) - 1\right] - J_L \quad (11)$$

where J_0 is the reverse saturation current, J_L is the photogenerated current, q is the elementary charge, k the Boltzmann constant, T the absolute temperature and A the ideality factor. The values of J_o and A are taken from reference [29].

The solar cell efficiency can be expressed by:

$$\eta = \frac{FF \times J_{SC} \times V_0}{P_{in}} \quad (12)$$

where FF is the fill factor, V_0 is the open circuit voltage, P_{in} is the density of the total solar radiation power at AM 1.5.

The fill factor can be written as:

$$FF = \frac{J_m \times V_m}{J_{SC} \times V_0} \quad (13)$$

where J_m and V_m are the maximum current density and voltage, respectively.

3. Results and discussion

Fig. 2 shows the dependence of short-circuit current density (J_{SC}) on ZnS content (x) and the corresponding optical losses.

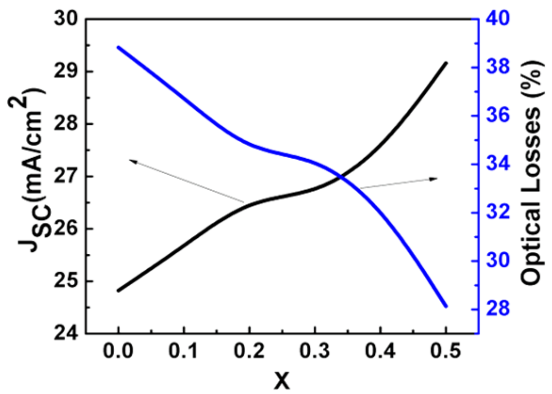

Fig. 2. Short-circuit current density (J_{SC}) and the corresponding optical losses for $(CdS)_{1-x}(ZnS)_x$/CIGS solar cell for x=0, 0.1, 0.2, 0.3, 0.4 and 0.5 (color online)

The calculations are carried out on the basis of the reflection losses at various interfaces and the absorption losses on both TCO layer (ZnO:Al) and buffer layer (CdS:ZnS). These calculations ignore the influence of the recombination losses.

It is clear that, J_{SC} increases with increasing the content of ZnS on $(CdS)_{1-x}(ZnS)_x$. Where J_{SC} increases from 24.8 mA/cm2 for pure CdS (x=0) to 29.2 mA/cm^2 for x = 0.5. Such increase in J_{SC} can be attributed to the increase of energy gap of the buffer layer with increasing the content of ZnS. More photons will pass through the buffer layer without absorption inside and reach at the absorber layer (CIGS) [30]. This can be understood from the variation of the optical losses with increasing x values. It can be seen that the optical losses decrease from 39% for x=0 to 28% for x=0.5. This indicates that when the ratio of addition of ZnS reaches 50% of the buffer layer, this leads to an increase in J_{SC} by 18% and a decrease in optical losses by more than 25%. In order to obtain real information about the performance of the solar cell, this requires taking into account the effect of the recombination loss that takes place during the generation of photocurrent. In this work we investigated the front recombination losses that occur at buffer layer/absorber layer interface and the back recombination losses that occur at absorber layer/back contact interface. The values of JSC under the influence of both optical and recombination losses are calculated and plotted in Fig. 3.

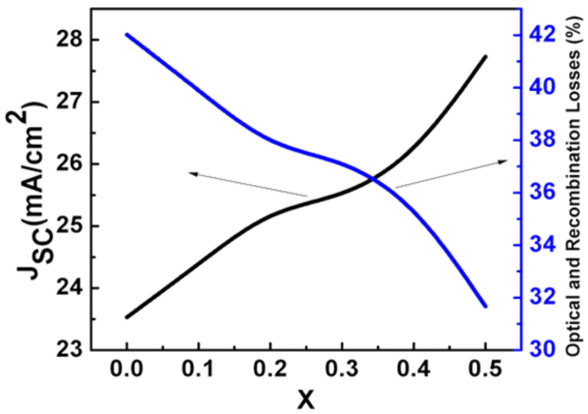

Fig. 3. Short-circuit current density (J_{SC}) and the corresponding optical and recombination losses for $(CdS)_{1-x}(ZnS)_x$/CIGS solar cell for x=0, 0.1, 0.2, 0.3, 0.4 and 0.5 (color online)

As seen in this figure, more reduction in J_{SC} can be observed when the recombination losses are taken into our account, where J_{SC} records 23.53 mA/cm^2 for x=0 and reaches 27.72 mA/cm^2 for x=0.5. On the other hand, the optical and recombination losses decrease from 42 % to 31.6 % for x= 0 and 0.5, respectively. Comparing the results from this figure with those obtained from Fig.2, we can conclude that the optical losses have significant effect on J_{SC} more than the effect of recombination losses.

The *J-V* curve of $(CdS)_{1-x}(ZnS)_x$/CIGS solar cell for x=0, 0.1, 0.2, 0.3, 0.4 and 0.5 is shown in Fig.4. With increasing the x-ratio, the curves are shifted downward due to the increase of J_{SC}. Many parameters namely; maximum voltage (V_m), maximum current density (J_m), open circuit voltage (V_O), fill factor (*FF*) and maximum power can be determined from *J-V* curve. These values are listed in Table 2 as a function of ZnS ratio (x).

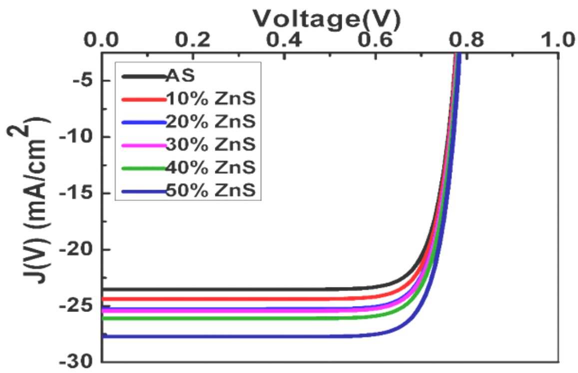

Fig. 4. J-V curves of $(CdS)_{1-x}(ZnS)_x$/CIGS solar cell for x=0, 0.1, 0.2, 0.3, 0.4 and 0.5 (color online)

Table 2. Maximum voltage (V_m), maximum current density (J_m), open circuit voltage (V_O), fill factor (FF) and cell power density (P_{max}) as a function of x-ratio for $(CdS)_{1-x}(ZnS)_x$/CIGS solar cell

x-ratio	V_m (mv)	J_m (mA/cm^2)	V_O (mv)	*FF* (%)	P_{max} (mW/cm^2)
0	685	21.52	780	80.2	14.74
0.1	685	22.43	781	80.7	15.36
0.2	685	23.29	781.5	80.8	15.95
0.3	685	23.58	782	81.1	16.15
0.4	685	24.15	785	80.7	16.54
0.5	685	25.87	787	81.1	17.72

The cell efficiency has been calculated using Eq. 12 and plotted in Fig. 5 as a function of x-ratio. From this figure it is noticed that the efficiency increases from 14.7% for pure CdS and reaches 17.72 % for x=0.5. This increase in CIGS solar cell efficiency is attributed mainly to the increase of J_{SC}.

The present work represents higher performance of the cell parameters compared to other experimental published results [31, 32]. On the other hand, our results is considered lower than this obtained theoretically by Abdalmageed et al. [33]. Where they achieved high conversion efficiency of 22 %. This big difference in the efficiency of solar cells can be due to neglecting of some losses that occur during the generation of photocurrent.

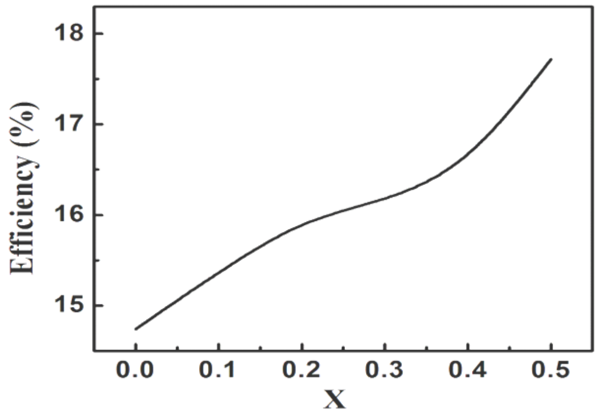

Fig. 5. The efficiency of $(CdS)_{1-x}(ZnS)_x$/CIGS solar cell for x=0, 0.1, 0.2, 0.3, 0.4 and 0.5

4. Conclusions

In this work, the effect of $(CdS)_{1-x}(ZnS)_x$ (x=0, 0.1, 0.2, 0.3, 0.4 and 0.5) on the performance of CIGS solar cells has been studied theoretically. The short-circuit current density, open-circuit voltage, fill factor cell power density and the cell efficiency were estimated. The calculations of these parameters are carried out on the basis of the optical properties of (CdS):(ZnS) buffer layer with different ZnS contents. The optical losses resulting from the reflection at different interfaces and absorption in TCO and buffer layers are taken into calculations. The recombination losses at front and back surface of CIGS are studied too. With increasing x-ratio, the short-circuit current density increased and both the optical and recombination losses decreased. Most of the losses were due to the optical losses. The efficiency of CIGS solar cells increased from 14.7% to 17.72% with increasing x-ratio from 0 to 0.5, respectively. This increase in CIGS solar cell efficiency is attributed mainly to the increase of J_{SC} and V_O.

References

[1] R. F. Service, Science **309**, 548 (2005).
[2] Z. L. Wang, J. H. Song, Science **312**, 242 (2006).
[3] G. W. Crabtree, N. S. Lewis, Physics Today **60**, 37 (2007).
[4] N. S. Lewis, Science **315**, 798 (2007).
[5] Renewable energy facts, Natural Resources Canada, 04-Jan-2018. [Online]. Available: http://www.nrcan.gc.ca/energy/facts/ renewableenergy/20069. [Accessed: 26-Feb-2018].
[6] T. M. Razikov, C. S. Ferekides, D. Morel, E. Stefanakos, H. S. Ullal, H. M. Upadhyaya, Solar Energy **85**, 1580 (2011).
[7] A. Goetzberger, C. Hebling, Solar Energy Materials and Solar Cells **62**, 1 (2000).
[8] A. Goodrich and M. Woodhouse, PV Manufacturing Cost Analysis: Future Cost Reduction Opportunities, 2012.
[9] W. U. Huynh, J. J. Dittmer, A. P. Alivisatos, Science **295**, 2425 (2002).
[10] H Movla, Optik **124**, 5871 (2013).
[11] T. Wada, Y. Hashimoto, S. Nishiwaki, T. Satoh, S. Hayashi, T. Negami, H. Miyake, Solar Energy Materials and Solar Cells **67**, 305 (2001).
[12] H. Heriche, Z. Rouabah, N. Bouarissa, Int. J. Hydrogen Energ. **42**, 9524 (2017)
[13] http://www.nrel.gov/ncpv/images/efficiency_chart.jpg
[14] L. A. Kosyachenko, X. Mathew, P. D. Paulson, V. Ya. Lytvynenko, O. L. Maslyanchuk, Solar Energy Materials and Solar Cells **130**, 291 (2014).
[15] F. L. Alvarado, J. A. Chavez, O. V. Galan, E. S. Meza, E. L. Chavez, G. C. Puente, Thin Solid Films **518**, 1796 (2010).
[16] H. Goto, Y. Hashimoto, K. Ito, Thin Solid Films **451-452**, 552 (2004).
[17] N. G. Dhere, A. A. Kadam, A. H. Jchagirdar, S. S. Kulkarni, L. Weinhardt, D. Grob, C. Heske, E. Umbach, Journal of Physics and Chemistry of Solids **66**, 1872 (2005).
[18] J. Han, G. Fu, V. Krishnakumar, C. Liao, W. Jaegermann, M. P. Besland, Journal of Physics and Chemistry of Solids **74**, 1879 (2013).
[19] T. Iwashita, S.Ando, Thin Solid Films **520**, 7076 (2012).
[20] Mahrous R. Ahmed, H. A. Mohamed, Sh. S. Ali, W. S. Mohamed, Physica B: Physics of Condensed Matter **612**, 412903 (2021).
[21] H. A. Mohamed, J. Appl. Phys. **113**, 093105 (2013).
[22] H. A. Mohamed, Mahrous R. Ahmed, Sh. S. Ali, W. S. Mohamed, Int. J. Thin. Film. Sci. Tec. **9**(3), 175 (2020).
[23] Q. Xu, R. D. Hong, H. L. Huang, Z. F. Zhang, M. K. Zhang, X. P. Chen, Z. Y. Wu, Opt. Laser Technol. **45**, 513 (2013).
[24] L. Kosyachenko, T. Toyama Solar Energy Materials and Solar Cells **120**, (5122014).
[25] L. A. Kosyachenko, Semiconductors **40**, 710 (2006).
[26] S. M. Sze, K. K. Ng, Physics of Semiconductor Devices, 3rd ed., Wiley- Interscience, New Jersey, 2006.
[27] L. A. Kosyachenko, X. Mathew, P. D. Paulson, V. Ya. Lytvynenko, O. L. Maslyanchuk, Solar

Energy Materials and Solar Cells **130**, 291 (2014).
[28] H. A. Mohamed, A. S. Mohamed, H. M. Ali, Mater. Res. Express **5**, 056411 (2018).
[29] W. Wang, M. T. Winkler, O. Gunawan, T. Gokmen, T. K. Todorov, Y. Zhu, D. B. Mitzi, Adv. Energy Mater. **4**, 1301465 (2014)
[30] L. A. Kosyachenko, X. Mathew, V. Ya.Roshko, E. V. Grushko, Solar Energy Materials and Solar Cells **114**, 179 (2013).
[31] M. M. Islam, S. Ishizuka, A. Yamada, K. Sakurai, S. Niki, T. Sakurai, K. Akimoto, Solar Energy Materials and Solar Cells **93**(6-7), 970 (2009).
[32] Jia-Show Ho, Shih-Cheng Chang, Jyh-Jier Ho, Wei-Tse Hsu, Chien-Chih Chiang, Materials Science in Semiconductor Processing **59**, 29 (2017).
[33] Hassan Ismail Abdalmageed, Mostafa Fedawy, Moustafa H. Aly, Journal of Physics: Conference Series, IOP Publishing, 012009 (2021).

*Corresponding author: hussein_abdelhafez2000@yahoo.com